Mineralogical Magazine, December 2009, Vol. 73(6), pp. 1033–1050

The crystal chemistry of holtite

L. A. GROAT[1,*], E. S. GREW[2], R. J. EVANS[1], A. PIECZKA[3] AND T. S. ERCIT[4]

[1] Department of Earth and Ocean Sciences, University of British Columbia, 6339 Stores Road, Vancouver, British Columbia V6T 1Z4, Canada
[2] Department of Earth Sciences, University of Maine, 5790 Bryand Global Sciences Center, Orono, Maine 04469-5790, USA
[3] Department of Mineralogy, Petrography, and Geochemistry, AGH-University of Science and Technology, Mickiewicza 30, 30-059 Kraków, Poland
[4] Canadian Museum of Nature, Research Division, Ottawa, Ontario K1P 6P4, Canada

[*Received 26 July 2009; Accepted 22 December 2009*]

ABSTRACT

Holtite, approximately $(Al,Ta,\square)Al_6(BO_3)(Si,Sb^{3+},As^{3+})_{\Sigma3}O_{12}(O,OH,\square)_{\Sigma3}$, is a member of the dumortierite group that has been found in pegmatite, or alluvial deposits derived from pegmatite, at three localities: Greenbushes, Western Australia; Voron'i Tundry, Kola Peninsula, Russia; and Szklary, Lower Silesia, Poland. Holtite can contain >30 wt.% Sb_2O_3, As_2O_3, Ta_2O_5, Nb_2O_5, and TiO_2 (taken together), but none of these constituents is dominant at a crystallographic site, which raises the question whether this mineral is distinct from dumortierite. The crystal structures of four samples from the three localities have been refined to $R_1 = 0.02-0.05$. The results show dominantly: Al, Ta, and vacancies at the Al(1) position; Al and vacancies at the Al(2), (3) and (4) sites; Si and vacancies at the Si positions; and Sb, As and vacancies at the Sb sites for both Sb-poor (holtite I) and Sb-rich (holtite II) specimens. Although charge-balance calculations based on our single-crystal structure refinements suggest that essentially no water is present, Fourier transform infrared spectra confirm that some OH is present in the three samples that could be measured. By analogy with dumortierite, the largest peak at 3505–3490 cm^{-1} is identified with OH at the O(2) and O(7) positions. The single-crystal X-ray refinements and FTIR results suggest the following general formula for holtite: $Al_{7-[5x+y+z]/3}(Ta,Nb)_x\square_{[2x+y+z]/3}BSi_{3-y}(Sb,As)_yO_{18-y-z}(OH)_z$, where x is the total number of pentavalent cations, y is the total amount of Sb + As, and $z \leqslant y$ is the total amount of OH. Comparison with the electron microprobe compositions suggests the following approximate general formulae $Al_{5.83}(Ta,Nb)_{0.50}\square_{0.67}BSi_{2.50}(Sb,As)_{0.50}O_{17.00}(OH)_{0.50}$ and $Al_{5.92}(Ta,Nb)_{0.25}\square_{0.83}BSi_{2.00}(Sb,As)_{1.00}O_{16.00}(OH)_{1.00}$ for holtite I and holtite II respectively. However, the crystal structure refinements do not indicate a fundamental difference in cation ordering that might serve as a criterion for recognizing the two holtites as distinct species, and anion compositions are also not sufficiently different. Moreover, available analyses suggest the possibility of a continuum in the Si/(Sb + As) ratio between holtite I and dumortierite, and at least a partial continuum between holtite I and holtite II. We recommend that use of the terms holtite I and holtite II be discontinued.

KEYWORDS: holtite, dumortierite, crystal chemistry, discontinued, Western Australia, Kola Peninsula, Lower Silesia.

Introduction

HOLTITE, approximately $(Al,Ta,\square)Al_6(BO_3)(Si,Sb^{3+},As^{3+})_{\Sigma3}O_{12}(O,OH,\square)_{\Sigma3}$, is a member of the dumortierite group that has been found in pegmatite, or alluvial deposits derived from pegmatite, at three localities: Greenbushes, Western Australia (Pryce, 1971; Hoskins *et al.*, 1989); Voron'i Tundry, Kola Peninsula, Russia (Voloshin *et al.*, 1977, 1987; Voloshin and Pakhomovskiy 1988); and Szklary, Lower

* E-mail: lgroat@eos.ubc.ca
DOI: 10.1180/minmag.2009.073.6.1033

Silesia, Poland (Pieczka and Marszałek, 1996). In addition to several distinctive structural features, such as face-sharing Al-octahedra and both cation and anion vacancies, holtite and dumortierite are unique among aluminosilicate minerals because they incorporate substantial amounts of the trace elements Nb, Ta, As and Sb, which generally form oxides, arsenates or sulphides rather than silicates in pegmatites and other deposits where such rare elements are concentrated. Unlike the situation for many new minerals described in the last 50 years, none of the four constituents that distinguish holtite from dumortierite is dominant at a specific crystallographic site, i.e. Si is dominant over Sb^{3+} and As^{3+} at the two tetrahedral sites and Al is dominant over Ta, Nb and vacancy at the Al(1) site in both minerals. Moreover, the term holtite has been applied to an ever-widening compositional range that blurred its distinction from dumortierite, which in turn has recently been found to contain significant Nb, Ta, As, Sb and Bi, further muddying the distinction (Groat *et al.*, 2001; Cempírek and Novák, 2004; Borghi *et al.*, 2004**;** Vaggelli *et al.*, 2004).

The primary objective of the present study is to obtain a better understanding of the structural features of holtite and the crystallographic role played by Nb, Ta, As, Sb and Bi in both holtite and dumortierite. A secondary objective is to consider the implications of our findings for clarifying the distinction between holtite and dumortierite.

Brief history of holtite

Holtite was first identified by Pryce (1971) in specimens from an alluvial tin deposit, derived from the weathering of pegmatite, near the township of Greenbushes, Western Australia (Pryce and Chester, 1978). Weissenberg photographs of single crystals gave space group *Pnma*, the same as dumortierite, and indicated the mineral had a crystal structure like dumortierite. However, chemical analyses showed, that in addition to major Al_2O_3 and SiO_2 and subordinate B_2O_3, holtite contains 18.0 wt.% Sb as Sb_2O_3 (originally reported as 4.61 wt.% Sb_2O_5 and 13.89 wt.% Sb_2O_3), 11.24 wt.% Ta_2O_5 and 0.76 wt.% Nb_2O_5, constituents not reported in dumortierite at that time (e.g. Grew, 1996).

Voloshin *et al.* (1977) described a second occurrence of holtite in a pegmatite at Mount Vasin-Myl'k, Voron'i Tundry, Kola Peninsula, Russia (specific locality from Pekov, 1998). The Voron'i Tundry holtite was reported to contain more SiO_2 (26.6–26.7 wt.% *vs*. 20.3 wt.% by wet chemistry) than the type material, but only a third of the Sb (5.8–6.4 wt.% *vs*. 18.0 wt.% as Sb_2O_3), i.e. it was intermediate in composition between type holtite and dumortierite. Moreover, Voloshin *et al.* (1977) reported 2.5–3.2 wt.% As_2O_3 and a B_2O_3 content (4.7–5.1 wt.%) approaching the ideal value consistent with the dumortierite structure; cf. 1.8 wt.% in the type holtite, which Hoskins *et al.* (1989) suggested was in error as the structure refinement gave stoichiometric B. In a more detailed study of the Voron'i Tundry material, Voloshin *et al.* (1987) recognized two varieties of holtite: low-Sb holtite I, an early-formed phase, which was described in 1977, and high-Sb holtite II, a late-formed phase. The latter had SiO_2 and Sb (as Sb_2O_3) contents close to those of the type material; it also contained As, which Voloshin *et al.* (1987) also found in a sample from Greenbushes.

Pieczka and Marszałek (1996) described a third holtite occurrence in a pegmatite in Szklary, Lower Silesia, Poland. Containing 12.9 wt.% Sb (as Sb_2O_3), this holtite appeared to be yet another intermediate, but when As is added to Sb (see below), this holtite is close to holtite II and type holtite in Si and (Sb^{3+}+ As^{3+}) content. However, its Ta_2O_5 content of 5.1 wt.% is but half that of the other three holtites, i.e. 9.8–14.5 wt.% (Pryce, 1971; Voloshin *et al.*, 1977, 1987; Voloshin and Pakhomovskiy 1988).

Groat *et al.* (2002) found both varieties of holtite in samples from Greenbushes, leaving Szklary the only locality where but one variety had been found. Kazantsev *et al.* (2005) concluded that the absence of any intermediate compositions allows one to consider the two varieties as independent with the main difference between the two being the Si:(Sb+As) ratio: 8.5:1.5 in holtite I and 7:3 in holtite II, and by extension, 10:0 in dumortierite. However, T.S. Ercit contended in Locock *et al.* (2006) that the terms holtite I and holtite II are paragenetic-compositional varietal names for holtite with inferred, but not proven, structural differences. Ercit also pointed out that the varietal distinction is based on amounts of Sb and As subordinate to the Si they replace, and that this terminology has not been approved by the Commission on New Minerals, Nomenclature and Classification of the International Mineralogical Association (CNMNC IMA). In summary, one is left with the impression that the name holtite has become a

'catch-all' term for pegmatitic dumortierite-like minerals containing significant Sb, As, Ta and Nb, rather than a mineral with a well defined composition.

In claiming that Sb is absent in dumortierite, Kazantsev *et al.* (2005) was ignoring recent chemical data on this mineral. Groat *et al.* (2001) reported up to 1.0 wt.% Sb_2O_3 in dumortierite from localities worldwide. Borghi *et al.* (2004) and Vaggelli *et al.* (2004) analysed zoned dumortierite in quartzites from Mozambique in which Sb_2O_3 ranged from 0 to 4.5 wt.% and varied inversely with Si. The Sb-rich cores are closer in Sb content to holtite I than to Sb-free dumortierite, and the zoning suggests the possibility of complete solid solution between holtite I and dumortierite. That is, holtite I might be better classed as Sb-Ta-As rich dumortierite, leaving open the question whether holtite II is a species distinct from dumortierite.

Previous structure studies

Hoskins *et al.* (1989) solved and refined the crystal structure of a Greenbushes crystal to R = 0.030 in space group *Pnma*. They determined that the crystal structure is closely related to that of dumortierite, which was described by Golovastikov (1965) and Moore and Araki (1978) as a design on the semi-regular planar net {6·4·3·4}. Moore and Araki (1978) showed that the net can be broken down into four regions:
(1) [AlO_3] chains of face-sharing octahedra (the Al(1) sites) with circumjacent 'pinwheels' of six SiO_4 tetrahedra, two Si(1) and four Si(2) sites;
(2) [Al_4O_{12}] cubic close-packed chains, containing the Al(2) and Al(3) octahedral sites, that are joined to equivalent chains by reflection at the O(1) corners of the Al(2) octahedra to form [Al_4O_{11}] sheets oriented parallel to (010);
(3) [Al_4O_{12}] double chains containing the Al(4) octahedral sites;
(4) BO_3 triangles (Fig. 1).

The Al(1)–Al(1) distance is ~2.35 Å, which is unusually short for face-sharing octahedra, and the Al(1) site is on average 75% occupied (Moore and Araki, 1978). The Al(1) face-sharing chains are disordered, which results in an average chain length that can be adjusted to fit the repeat distance of the remaining octahedral framework in the structure (Moore and Araki, 1978).

Hoskins *et al.* (1989) showed that the crystal structure of holtite differs from that of dumortierite in several important respects, all of which

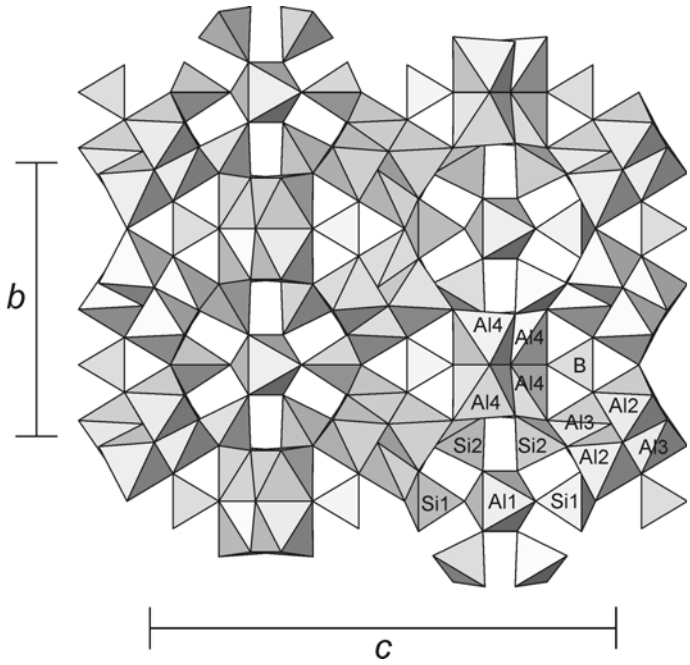

FIG. 1. The structure of dumortiertite observed along the *a* axis.

lie within the first region of Moore and Araki (1978), i.e. within six-sided tunnels bounded by the two regions composed of $[Al_4O_{12}]$ chains. Both SiO_4 tetrahedra are partially replaced by $Sb^{3+}O_3$ triangular pyramids with no evidence of preference of Sb for one or other of the Si sites, and with Ta replacing Al at the Al(1) position (Fig. 2). As a result, there are vacancies at the coordinating anion sites [O(2) and O(7)] as well as at the Al(1) site. Relative to the Si positions, the Sb^{3+} sites are shifted about 0.5 Å closer to the Al(1) position to accommodate the longer Sb^{3+}–anion bonds (average ~1.9 Å). When the Sb sites are occupied, the adjacent Si, O(2) [for Si(1)], and O(7) [for Si(2)] positions are vacant. Hoskins *et al.* (1989) obtained the formula $(Si_{2.25}Sb_{0.75})B[Al_6(Al_{0.43}Ta_{0.27}\square_{0.30})O_{15}(O,OH)_{2.25}]$ (Z = 4) from their crystal-structure study.

Both Pryce (1971) and Hoskins *et al.* (1989) reported diffuse layers normal to *a* at spacings of 2*a* and 3*a* in rotation photographs of holtite. Hoskins *et al.* (1989) suggested that the diffuse layers visible in the photographs indicated that although there is an ordering effect in any one individual tunnel, it is not strongly correlated with that of adjacent tunnels. They went on to suggest that a complete replacement of SiO_4 rings by SbO_3 rings takes place at ordered intervals, which are likely related to the order of the vacancies at the Al(1) site.

Kazantsev *et al.* (2005, 2006) refined the crystal structure of an As-bearing holtite I crystal from Voron'i Tundry to R = 0.046. They reported that As^{3+} is incorporated into the crystal structure in $(Sb,As)O_3$ pyramids, substituting for SiO_4 tetrahedra just as SbO_3 pyramids substitute for SiO_4 tetrahedra in holtite from Greenbushes, and that there was no preference for either of the two Si positions. Kazantsev *et al.* (2006) derived the following chemical formula from their crystal structure study: $(Al_{0.61}Ta_{0.25}\square)(Al_{0.96}\square)_2(Al_{0.96}\square)_2(Al_{0.90}\square)_2(Si_{2.49}Sb_{0.35}As_{0.13})O_{13.46}(O_{0.48}OH_{0.52})(BO_3)$.

Using the Rietveld method, Zubkova *et al.* (2006) refined the crystal structure of a Voron'i Tundry holtite II from powder data (to Rp = 2.93% and Rb = 2.10%) and found that the crystal structure differs from those of holtite I and of the Greenbushes holtite (Hoskins *et al.*, 1989), which is also holtite II, in that the Si(1) position is vacant, the Sb(1) position is only partially occupied and approximately 5% of the Al atoms at the Al(2) site are replaced by Sb^{5+} cations, giving $(Ta_{0.30}Al_{0.26}\square)(Al_{0.95}Sb^{5+}_{0.05})_2Al_2(Al_{0.98}\square)_2(Si_{0.65}Sb^{3+}_{0.30}As_{0.05})_3(Sb^{3+}_{0.44}\square)O_{9.30}(O,OH)_{4.56}(BO_3)$. The refined Si content is about two thirds of that measured by electron microprobe, a discrepancy that Zubkova *et al.* (2006) attributed to contamination by quartz and amorphous silica encasing the studied holtite fibres. However, the measured SiO_2 is 17.31 wt.% (Kazantsev *et al.*, 2005), a value typical of holtite II.

Experimental

Preliminary examination of samples from all three localities with a Philips XL30 scanning electron microscope equipped with an energy-dispersion

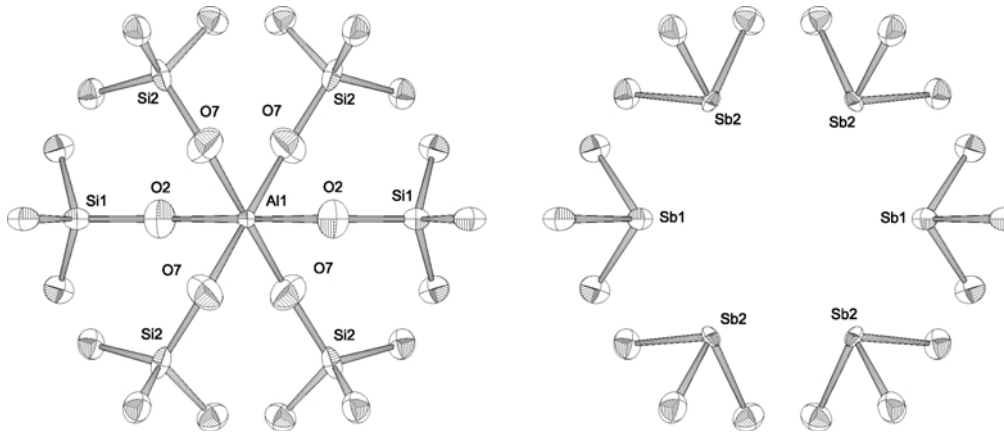

FIG. 2. Disposition of SiO_4 tetrahedra (left) and $(Sb,As)O_3$ groups (right) and the coordinated central Al(1) site in holtite (after Hoskins *et al.*, 1989).

X-ray spectrometer revealed holtite I in the sample from Voron'i Tundry (labelled H1), holtite II in the specimen from Szklary (H4), and both holtite I and holtite II in the sample from Greenbushes (H2 and H3).

For the X-ray experiments, crystals of samples H1–3 were ground to approximate spheres with a Nonius sphere grinder. This was not possible for H4, which has a fibrous habit, so a single fibre was carefully extracted from the mass. Single-crystal X-ray diffraction measurements were made at C-HORSE (the Centre for Higher Order Structure Elucidation, in the Department of Chemistry at UBC) using a Bruker X8 APEX II diffractometer with graphite monochromated Mo-$K\alpha$ radiation. Data were collected in a series of ϕ and ω scans in 0.50º oscillations with 10.0 second exposures. The crystal-to-detector distance was 40 mm. Data were collected and integrated using the Bruker *SAINT* software package. Data for samples H1–3 were corrected for absorption effects using the multi-scan technique (*SADABS*) and were corrected for Lorentz and polarization effects. Examination of the data for the H4 samples showed that the crystal is made up of three twin individuals related by 120º rotation about a threefold twin axis parallel to *a*. The data were resolved using *CELL NOW* and were corrected for absorption effects using *TWINABS* and then for Lorentz and polarization effects.

All refinements were performed using the *SHELXTL* crystallographic software package of Bruker AXS. The structures were refined using starting parameters from Hoskins *et al.* (1989). Scattering factors for neutral atoms were used for the cations, and ionic factors for O^{2-} for oxygen. All atoms were refined anisotropically. The weighting scheme was based on counting statistics. Neutral atom scattering factors were taken from Cromer and Waber (1974). Anomalous dispersion effects were included in $F_{calc.}$ (Ibers and Hamilton, 1964); the values for $\Delta f'$ and $\Delta f''$ were those of Creagh and McAuley (1992). The values for the mass attenuation coefficients are those of Creagh and Hubbell (1992). The following assumptions were made and appropriate constraints applied:

(1) The Si(1) and Si(2) sites were assumed to contain only silicon atoms or be vacant. When occupied, the sites were assumed to be coordinated by four O atoms in tetrahedral coordination. The O(2) and O(7) sites were assumed to contain only oxygen atoms or be vacant. The occupancies of all four sites were constrained to be equivalent (taking into account the different multiplicities of the sites).

(2) A cation was assumed to occupy the Al(1) site when there were oxygen atoms at the coordinating O(2) and O(7) positions. Therefore, the atomic occupancy of the Al(1) site was fixed at the value obtained through refinement for the O(2) and O(7) (and hence Si(1) and Si(2)) sites.

(3) The ratio of Al:Ta was refined within this overall fixed value.

(4) The Sb(1) site was assumed to be coordinated by three O atoms in trigonal coordination, and to be occupied when the Si(1) site was empty; the same assumptions were made for the Sb(2) and Si(2) sites. The overall occupancy of the Sb(1) and Sb(2) sites was fixed at values inverse of those refined for the Si(1) and Si(2) [and O(2) and O(7)] sites.

(5) The ratio of Sb:As was refined within this overall fixed value.

(6) When necessary, the overall occupancies of the Al(1), Sb(1) and Sb(2) sites were adjusted to match the refined occupancies of the Si(1), Si(2), O(2) and O(7) sites.

(7) The occupancies of the Al(2), Al(3) and Al(4) sites were refined.

Moore and Araki (1978) and Alexander *et al.* (1986) suggested that the apparent partial occupancies of the Al(2), Al(3) and Al(4) sites in dumortierite were due to a correlation between site occupancies and thermal motion. Alexander *et al.* (1986) therefore scaled the refined occupancies of the Al(2–4) sites by dividing them by 0.95. However, Ferraris *et al.* (1995) suggested that for their refinement of the crystal structure of magnesiodumortierite there was no valid reason to disregard the refined values. In our study, constraining these sites to be fully occupied with Al resulted in increases in the *R* values by at least 1%, and attempts to refine for cations in addition to Al (such as Ti) were unsuccessful.

After collection of X-ray diffraction data, the single crystals were attached to Lucite disks with Petropoxy and polished for the electron microprobe study. In order to obtain the most accurate possible compositions, electron microprobe data were collected from all of the crystals (except H2) using two different instruments, one at University of British Columbia (UBC) and the other at the Canadian Museum of Nature (CMN).

At UBC, compositions were obtained with a fully-automated Cameca SX50 microprobe, operating in the wavelength-dispersion mode with the following operating conditions: excitation

voltage, 20 kV; probe current, 20 nA; peak count time, 20 s; background count time, 10 s; final beam diameter, 10 μm. Data reduction was carried out with the "PAP" $\phi(\rho Z)$ method (Pouchou and Pichoir, 1985). For the elements considered, the following standards and X-ray lines were used: kyanite, Al-$K\alpha$, Si-$K\alpha$; apatite, P-$K\alpha$; rutile, Ti-$K\alpha$; synthetic fayalite, Fe-$K\alpha$; tennantite, As-$K\alpha$; columbite, Nb-$L\alpha$; tetrahedrite, Sb-$L\alpha$; microlite, Ta-$M\alpha$.

At CMN, compositions were obtained with a JEOL 733 electron microprobe with Geller automation, operating in the wavelength-dispersion mode with the following operating conditions: excitation voltage, 15 kV; probe current, 20 nA; peak count time, 50 s; background count time, 25 s; final beam diameter, 10 μm. Data reduction was carried out with the "PAP" $\phi(\rho Z)$ method (Pouchou and Pichoir, 1985) and was checked with *CITZAF* (Armstrong, 1995). For the elements considered, the following standards and X-ray lines were used: kyanite, Al-$K\alpha$, Si-$K\alpha$; apatite, P-$K\alpha$; rutile, Ti-$K\alpha$; hematite, Fe-$K\alpha$; GaAs, As-$L\alpha$; stibiotantalite, Nb-$L\alpha$, Sb-$L\alpha$, Ta-$M\alpha$.

Formulae were calculated from the electron microprobe data using the number of oxygen atoms determined from the X-ray refinements and assuming 1 B atom per formula unit (a.p.f.u.).

Fourier transform infrared spectroscopy (FTIR) was performed at the Canadian Conservation Institute on a holtite sample from Szklary (H4) and two from Greenbushes, one obtained from the Australian Museum of Mineralogy (sample

TABLE 1. Average electron microprobe compositions of holtite.

Sample	H1 Holtite I n = 11	H2 Holtite I n = 11	H3 Holtite II n = 2	H4 Holtite II n = 10
Wt.%				
P_2O_5	0.19	0.18	0.00	0.24
Nb_2O_5	0.21	0.18	0.05	1.12
Ta_2O_5	12.06	13.15	10.93	5.06
SiO_2	22.31	23.66	18.24	18.02
TiO_2	0.01	0.00	0.09	1.46
B_2O_3	5.12	5.20	4.98	5.20
Al_2O_3	46.20	46.85	43.50	47.62
Fe_2O_3	0.00	0.01	0.32	0.22
As_2O_3	3.35	2.33	2.80	3.86
Sb_2O_3	6.81	4.85	17.29	15.04
Total	96.26	96.41	98.20	97.84
P^{5+}	0.018	0.017	0.000	0.023
Nb^{5+}	0.011	0.009	0.003	0.056
Ta^{5+}	0.371	0.399	0.345	0.153
Si^{4+}	2.524	2.638	2.120	2.008
Ti^{4+}	0.001	0.000	0.008	0.122
B^{3+}	1	1	1	1
Al^{3+}	6.160	6.156	5.959	6.255
Fe^{3+}	0.000	0.001	0.028	0.018
As^{3+}	0.230	0.158	0.198	0.261
Sb^{3+}	0.318	0.223	0.828	0.691
As + Sb	0.548	0.381	1.026	0.952
Nb + Ta	0.382	0.408	0.348	0.209
O	17.610	17.643	17.145	17.180

Number of analyses used in average = n.
Mg sought but not detected.
Formulae were calculated using the number of oxygen atoms determined from the X-ray refinements and assuming 1 B a.p.f.u.

D43778, labelled A) and the other from the Smithsonian Institution (sample NMNH 128674, labelled S). The available amount of Voron'i Tundry material was insufficient for FTIR. Each sample was separated from the rock and washed with ethanol. The sample was positioned on a Spectra-Tech low-pressure diamond microsample cell and analysed using a Bruker Optics Hyperion 2000 microscope interfaced to a Tensor 27 spectrometer. The spectrum was acquired in the 4000 to 430 cm^{-1} range by co-adding 150 scans.

Results

Average electron microprobe compositions of the structure crystals are given in Table 1. The totals are low, even if water is present. The (sub)microfibrous character of holtite is a possible cause of the low analytical totals. Grew *et al*. (2008) attributed low totals for analyses of finely porous material to contamination from epoxy filling the pores; similarly, epoxy could have filled the gaps between the very fine fibres of holtite. In addition, we suspect that the data reduction routines are unable to correct completely for the effect of As, Sb, and Ta on Si and Al, elements not normally analysed together. The results confirm that samples H1 and H2 are holtite I and H3 and H4 are holtite II, with a maximum of 17.29 wt.% Sb_2O_3 (0.82 Sb a.p.f.u.) in H3. The compositions also show 2.33−3.86 wt.% As_2O_3 (0.16−0.26 As a.p.f.u.) and, as expected, Si+As+Sb equals ~3 a.p.f.u. Samples H1, H2 and H3 contain similar amounts of Ta (0.34−0.40 Ta a.p.f.u.); H4 contains approximately half as much Ta (0.15 Ta a.p.f.u.) but considerably more Nb (0.06 a.p.f.u.) and Ti (0.12 a.p.f.u.). The compositions also show 43.50−47.62 wt.% Al_2O_3 (5.88−6.26 Al a.p.f.u.). Three of the samples also show traces of P (to 0.02 P a.p.f.u.).

Data collection and refinement parameters for the single-crystal X-ray experiments are summarized in Table 2, positional parameters in Table 3 and bond lengths in Table 4. A full list of atomic

TABLE 2. Data measurement and refinement information.

Specimen	H1	H2	H3	H4
a (Å)	4.6818(4)	4.6981(7)	4.6900(6)	4.7264(9)
b (Å)	11.867(1)	11.926(2)	11.897(4)	11.981(2)
c (Å)	20.302(2)	20.413(3)	20.385(6)	20.566(4)
V (Å^3)	1127.9(2)	1143.7(3)	1137.4(5)	1164.6(4)
Space Group	*Pnma*			
Z	4			
Crystal size (mm)	0.17 × 0.14 × 0.14	0.14 × 0.11 × 0.08	0.12 × 0.08 × 0.06	0.18 × 0.02 × 0.02
$D_{calc.}$ (Mg m^{-3})	4.916	4.848	4.875	4.762
Radiation	Mo-$K\alpha$			
Monochromator	Graphite			
Total F_o	29307	10309	3871	1215
Unique F_o	1754	1733	1741	1057
$F_o > 4\sigma F_o$	1693	1508	1439	826
R_{int}	0.03(1)	0.03(2)	0.03(3)	–
L.s. parameters	165	165	165	167
Range of h	$-6 \leqslant 6$	$-5 \leqslant 6$	$0 \leqslant 6$	$0 \leqslant 5$
Range of k	$-14 \leqslant 16$	$-15 \leqslant 16$	$0 \leqslant 16$	$-14 \leqslant 14$
Range of l	$-25 \leqslant 28$	$-25 \leqslant 28$	$-28 \leqslant 28$	$-24 \leqslant 24$
R_1 for $F_o > 4\sigma F_o$	0.0161	0.0172	0.0214	0.0511
R_1 for all unique F_o	0.0170	0.0238	0.0297	0.0795
wR_2	0.0411	0.0387	0.0446	0.1398
a	0.0142	0.0202	0.0183	0.0401
b	1.07	0.01	0.01	18.65
GoF (= S)	1.242	1.037	0.963	1.174
$\Delta\rho_{max}$ (e Å^{-3})	0.953	0.471	0.861	1.836
$\Delta\rho_{min}$ (e Å^{-3})	−0.525	−0.326	−0.429	−1.013

$w = 1/[\sigma^2(F_o^2) + (a'P)^2 + b'P]$ where $P = [\text{Max}(F_o^2, 0) + 2'F_c^2)]/3$

TABLE 3. Atomic parameters for holtite.

		H1	H2	H3	H4
Al(1)	x	0.40099(6)	0.40077(6)	0.40563(8)	0.4048(7)
	y	¾	¾	¾	¾
	z	0.25024(1)	0.25027(1)	0.24991(2)	0.2504(2)
	U_{eq}	0.01537(9)	0.01530(9)	0.0050(1)	0.030(1)
	n_{Al}	0.2753(5)	0.2799(5)	0.2291(5)	0.310(2)
	n_{Ta}	0.1597(5)	0.1618(5)	0.1304(5)	0.053(2)
Al(2)	x	0.55777(8)	0.55782(9)	0.5571(1)	0.5577(8)
	y	0.61051(3)	0.61049(3)	0.61078(5)	0.6107(3)
	z	0.47331(2)	0.47333(2)	0.47353(3)	0.4733(2)
	U_{eq}	0.0054(1)	0.0053(1)	0.0039(2)	0.012(1)
	n	0.986(3)	0.993(2)	0.994(4)	1.00(2)
Al(3)	x	0.05959(8)	0.05953(9)	0.0586(1)	0.0594(8)
	y	0.49029(3)	0.49028(3)	0.48992(5)	0.4893(3)
	z	0.43152(2)	0.43151(2)	0.43149(3)	0.4311(2)
	U_{eq}	0.0053(1)	0.0049(1)	0.0041(2)	0.010(1)
	n	0.984(3)	0.989(2)	0.992(4)	1.00(2)
Al(4)	x	0.06075(9)	0.0602(1)	0.0598(1)	0.0596(8)
	y	0.35985(4)	0.35952(4)	0.35925(5)	0.3577(3)
	z	0.29022(2)	0.29005(2)	0.29023(3)	0.2894(2)
	U_{eq}	0.0079(2)	0.0073(2)	0.0061(2)	0.013(1)
	n	0.916(3)	0.930(3)	0.971(4)	0.96(2)
Si(1)	x	0.0868(3)	0.0862(3)	0.0874(4)	0.089(4)
	y	¾	¾	¾	¾
	z	0.40833(7)	0.40839(6)	0.4079(1)	0.4080(7)
	U_{eq}	0.0054(2)	0.0050(2)	0.0033(3)	0.018(3)
	n	0.435(2)	0.442(2)	0.359(2)	0.363(5)
Sb(1)	x	0.1109(6)	0.1103(8)	0.1135(3)	0.113(3)
	y	¾	¾	¾	¾
	z	0.3861(2)	0.3865(2)	0.38349(8)	0.3864(4)
	U_{eq}	0.0107(6)	0.0103(8)	0.0067(3)	0.016(2)
	n_{Sb}	0.033(2)	0.028(2)	0.120(3)	0.11(1)
	n_{As}	0.032(2)	0.030(2)	0.021(3)	0.03(1)
Si(2)	x	0.5875(1)	0.5871(2)	0.5878(2)	0.591(2)
	y	0.5205(1)	0.52053(9)	0.5209(2)	0.5225(7)
	z	0.32972(4)	0.32979(4)	0.32970(6)	0.3295(4)
	U_{eq}	0.0055(2)	0.0054(2)	0.0041(2)	0.009(1)
	N	0.870(4)	0.883(3)	0.719(5)	0.73(1)
Sb(2)	x	0.6091(3)	0.6086(4)	0.6108(2)	0.610(1)
	y	0.5596(2)	0.5589(2)	0.5619(1)	0.5596(5)
	z	0.31736(8)	0.31747(9)	0.31676(4)	0.3171(4)
	U_{eq}	0.0089(4)	0.0093(5)	0.0060(2)	0.015(1)
	n_{Sb}	0.086(4)	0.077(3)	0.276(5)	0.20(1)
	n_{As}	0.044(4)	0.039(3)	0.005(5)	0.08(1)
B	x	0.2280(4)	0.2274(5)	0.2265(6)	0.234(4)
	y	¼	¼	¼	¼
	z	0.4156(1)	0.4155(1)	0.4160(2)	0.416(1)
	U_{eq}	0.0070(4)	0.0066(4)	0.0047(5)	0.017(3)
O(1)	x	0.3777(3)	0.3774(3)	0.3790(4)	0.376(2)
	y	¾	¾	¾	¾
	z	0.45681(7)	0.45674(7)	0.4573(1)	0.4566(6)
	U_{eq}	0.0072(3)	0.0063(3)	0.0057(4)	0.013(2)

Table 3 (*contd.*)

		H1	H2	H3	H4
O(2)	*x*	0.1613(4)	0.1613(4)	0.1622(7)	0.159(4)
	y	¾	¾	¾	¾
	z	0.33042(8)	0.33048(8)	0.3303(1)	0.3286(9)
	U_{eq}	0.0104(4)	0.0106(4)	0.0086(7)	0.022(3)
	n	0.435(2)	0.442(2)	0.359(2)	0.363(5)
O(3)	*x*	0.8943(2)	0.8943(2)	0.8914(3)	0.891(2)
	y	0.63873(8)	0.63880(8)	0.6380(1)	0.6381(6)
	z	0.42518(5)	0.42516(5)	0.42427(7)	0.4247(4)
	U_{eq}	0.0068(2)	0.0062(2)	0.0055(3)	0.013(2)
O(4)	*x*	0.4039(2)	0.4035(2)	0.4017(3)	0.401(2)
	y	0.43460(8)	0.43452(8)	0.4349(1)	0.4363(6)
	z	0.28240(5)	0.28251(5)	0.28166(7)	0.2824(4)
	U_{eq}	0.0082(2)	0.0073(2)	0.0062(3)	0.012(2)
O(5)	*x*	0.3942(2)	0.3944(2)	0.3918(3)	0.392(2)
	y	0.54999(8)	0.54984(8)	0.5507(1)	0.5513(6)
	z	0.39419(5)	0.39427(5)	0.39412(6)	0.3948(4)
	U_{eq}	0.0069(2)	0.0063(2)	0.0050(3)	0.010(1)
O(6)	*x*	0.8811(2)	0.8807(2)	0.8828(3)	0.886(1)
	y	0.45102(8)	0.45119(8)	0.4506(1)	0.4475(6)
	z	0.35231(5)	0.35208(5)	0.35194(6)	0.3518(4)
	U_{eq}	0.0078(2)	0.0070(2)	0.0060(3)	0.013(1)
O(7)	*x*	0.6585(3)	0.6586(3)	0.6607(4)	0.658(2)
	y	0.6333(1)	0.6333(1)	0.6331(2)	0.635(1)
	z	0.28894(6)	0.28880(6)	0.28848(9)	0.2880(6)
	U_{eq}	0.0116(3)	0.0108(3)	0.0086(6)	0.022(2)
	n	0.870(4)	0.883(3)	0.719(5)	0.73(1)
O(8)	*x*	0.1752(3)	0.1726(3)	0.1737(4)	0.178(3)
	y	¼	¼	¼	¼
	z	0.34978(7)	0.34990(7)	0.35013(9)	0.3498(6)
	U_{eq}	0.0100(3)	0.0087(3)	0.0071(4)	0.012(2)
O(9)	*x*	0.2539(2)	0.2537(2)	0.2540(3)	0.253(2)
	y	0.35050(8)	0.35049(8)	0.3506(1)	0.3504(8)
	z	0.44768(5)	0.44776(5)	0.44791(6)	0.4474(6)
	U_{eq}	0.0074(2)	0.0068(2)	0.0057(3)	0.018(2)
O(10)	*x*	0.7568(3)	0.7576(3)	0.7611(4)	0.769(2)
	y	¼	¼	¼	¼
	z	0.27390(7)	0.27364(7)	0.2732(1)	0.2730(8)
	U_{eq}	0.0109(3)	0.0102(3)	0.0080(4)	0.014(3)
O(11)	*x*	0.7501(2)	0.7500(2)	0.7500(3)	0.749(1)
	y	0.46706(8)	0.46710(8)	0.4673(1)	0.4683(7)
	z	0.48832(4)	0.48826(5)	0.48840(6)	0.4871(5)
	U_{eq}	0.0054(2)	0.0052(2)	0.0037(3)	0.007(2)

displacement parameters and bond angles (Tables S1 and S2 respectively), have been deposited with the Principal Editor of *Mineralogical Magazine* and are available from www.minersoc.org/pages/e_journals/dep_mat_mm.html. The very low *R* values for all of the samples except the twinned H4 crystal confirm that the refinement strategy outlined above is appropriate.

The average Al–O distances are remarkably similar for all four samples, at ~1.99 Å for <Al(1)–O> and 1.90–1.92 Å for <Al(2,3,4)–O>. However, the Al(4)–O(10) distances are appreciably longer than the average, at 1.92 to 2.07 Å.

TABLE 4. Interatomic distances (Å).

	H1	H2	H3	H4
Al(1)–O(2)	1.977(1)	1.987(2)	1.997(3)	1.98(2)
Al(1)–O(2)a	2.041(2)	2.053(2)	2.030(3)	2.02(2)
Al(1)–O(7)b,c ×2	1.959(1)	1.967(1)	1.966(2)	1.97(1)
Al(1)–O(7)d ×2	1.997(1)	2.006(1)	1.996(2)	1.99(1)
<Al(1)–O>	1.988	1.998	1.992	1.99
Al(2)–O(1)	1.8876(8)	1.8976(8)	1.884(1)	1.907(6)
Al(2)–O(3)	1.884(1)	1.892(1)	1.890(2)	1.894(9)
Al(2)–O(5)	1.919(1)	1.928(1)	1.932(2)	1.932(8)
Al(2)–O(9)e	1.888(1)	1.896(1)	1.887(2)	1.92(1)
Al(2)–O(11)e	1.879(1)	1.888(1)	1.882(1)	1.912(9)
Al(2)–O(11)	1.950(1)	1.958(1)	1.956(2)	1.952(9)
<Al(2)–O>	1.901	1.910	1.905	1.92
Al(3)–O(3)f	1.928(1)	1.938(1)	1.934(2)	1.958(8)
Al(3)–O(5)	1.879(1)	1.886(1)	1.883(2)	1.891(8)
Al(3)–O(6)f	1.871(1)	1.885(1)	1.878(2)	1.894(8)
Al(3)–O(9)	1.920(1)	1.929(1)	1.924(2)	1.93(1)
Al(3)–O(11)f	1.872(1)	1.879(1)	1.874(1)	1.882(9)
Al(3)–O(11)e	1.923(1)	1.934(1)	1.932(2)	1.98(1)
<Al(3)–O>	1.899	1.909	1.904	1.92
Al(4)–O(4)	1.842(1)	1.851(1)	1.847(2)	1.874(9)
Al(4)–O(4)b	1.871(1)	1.880(1)	1.873(2)	1.905(9)
Al(4)–O(6)f	1.862(1)	1.873(1)	1.858(2)	1.865(9)
Al(4)–O(8)	1.857(1)	1.865(1)	1.862(2)	1.876(9)
Al(4)–O(10)f	1.958(1)	1.960(1)	1.942(2)	1.92(1)
Al(4)–O(10)b	2.058(1)	2.063(1)	2.062(2)	2.07(1)
<Al(4)–O>	1.908	1.915	1.907	1.92
Si(1)–O(1)	1.680(2)	1.687(2)	1.699(3)	1.69(2)
Si(1)–O(2)	1.620(2)	1.629(2)	1.620(4)	1.66(2)
Si(1)–O(3)f,g ×2	1.635(1)	1.640(1)	1.653(2)	1.67(1)
<Si(1)–O>	1.643	1.649	1.656	1.67
Sb(1)–O(1)	1.903(3)	1.906(4)	1.954(2)	1.90(2)
Sb(1)–O(3)f,g ×2	1.844(2)	1.847(2)	1.885(2)	1.88(1)
<Sb–O>	1.864	1.867	1.908	1.89
Si(2)–O(4)	1.643(1)	1.651(1)	1.663(2)	1.68(1)
Si(2)–O(5)	1.629(1)	1.635(1)	1.642(2)	1.68(1)
Si(2)–O(6)	1.667(1)	1.672(1)	1.679(2)	1.72(1)
Si(2)–O(7)	1.609(2)	1.619(2)	1.614(3)	1.62(1)
<Si(2)–O>	1.637	1.644	1.650	1.68
Sb(2)–O(4)	1.904(2)	1.907(2)	1.938(2)	1.92(1)
Sb(2)–O(5)	1.860(2)	1.866(2)	1.886(2)	1.90(1)
Sb(2)–O(6)	1.945(2)	1.945(2)	1.973(2)	2.003(9)
<Sb–O>	1.903	1.906	1.932	1.94
B–O(8)	1.359(2)	1.364(2)	1.365(3)	1.39(3)
B–O(9)h ×2	1.364(1)	1.373(1)	1.368(2)	1.37(1)
<B–O>	1.362	1.370	1.367	1.38
Al(1)–Al(1) ×2	2.3409(2)	2.3491(4)	2.3450(3)	2.3633(5)
Si(1)–Sb(1)	0.465(3)	0.462(3)	0.512(1)	0.46(1)
Si(2)–Sb(2)	0.537(2)	0.532(2)	0.565(1)	0.520(5)

a: $x+\frac{1}{2}, y, -z+\frac{1}{2}$; b: $x-\frac{1}{2}, y, -z+\frac{1}{2}$; c: $x-\frac{1}{2}, -y+\frac{3}{2}, -z+\frac{1}{2}$; d: $x, -y+\frac{3}{2}, z$; e: $-x+1, -y+1, -z+1$; f: $x-1, y, z$; g: $x-1, -y+\frac{3}{2}, z$; h: $x, -y+\frac{1}{2}, z$.

According to Moore and Araki (1978) "...the Al4–O10 distance dilations can be easily explained by noting that all four Al cations surround and are practically coplanar to O10 and, therefore, exhibit uniform cation–cation repulsion away from central O10...". The distance dilations result in bond-valence totals of ~1.5 v.u. to the O(10) position. The Al(1)–Al(1) separation is similar for crystals H1, H2, and H3 (2.341–2.349 Å) but slightly longer for H4 (2.363 Å).

For the holtite I samples (H1 and H2), the refined occupancies of the Al(1) site were very similar at ~56% Al, 32% Ta and a 12% vacancy. For the holtite II sample H3, the Al(1) site occupancy refined to ~46% Al, 26% Ta, and a 28% vacancy. However, the refined Al(1) site occupancy for the other holtite II sample (H4) refined to 62% Al, 11% Ta, and a 27% vacancy. This probably reflects the presence of Ti and Nb, as shown by the electron microprobe compositions; studies of dumortierite (Alexander *et al.*, 1986; Platonov *et al.*, 2000) have shown that Ti substitutes at the Al(1) site, and we would expect Nb to do so also, based on its similarity in valence and radius to Ta. The occupancies of the Al(2) and Al(3) positions refined to between 98 and 100% Al for all of the samples studied. However, the occupancy of the Al(4) position was lower for the holtite I samples (92 and 93% Al for H1 and H2 respectively) than for the holtite II samples (96 and 97% Al for H3 and H4 respectively).

The average Si(1)–O and Si(2)–O distances are slightly shorter (1.64–1.65 and 1.64 Å respectively) for the holtite I samples than for the holtite II crystals (1.66–1.67 and 1.65–1.68 Å), reflecting the difference in Si site occupancies (88% in holtite I *vs.* 72% in holtite II). Similarly, the average Sb(1)–O and Sb(2)–O distances are shorter (1.86–1.87 and 1.90–1.91 Å respectively) for the holtite I phases than for the holtite II samples (1.89–1.91 and 1.93–1.94 Å).

The Si(1)–Sb(1) and Si(2)–Sb(2) separations are similar for the holtite I crystals (0.46–0.47 and 0.53–0.54 Å respectively) and longer for the holtite II crystal H3 (0.51 and 0.57 Å). The twinned holtite II crystal H4 shows a similar Si(1)–Sb(1) separation to the holtite I samples (0.46 Å) but the shortest Si(2)–Sb(2) distance (0.52 Å).

For the holtite I samples, the refined occupancies of the Si(1), Sb(1), Si(2) and Sb(2) sites were also very similar, at ~88% Si and 12% vacancies for the Si(1) and Si(2) sites, and ~12% Sb+As (6% Sb and 6% As at the Sb(1) site, and 8% Sb and 4% As at the Sb(2) site) and 88% vacancies for the Sb(1) and Sb(2) positions.

For the holtite II samples, the Si(1) and Si(2) positions showed refined occupancies of ~72% Si and 28% vacancies. The Sb(1) and Sb(2) site occupancies refined to ~28% vacancies, therefore the Sb(1) and Sb(2) occupancies are 28% Sb+As and 72% vacancies, but the relative amounts of Sb and As were different for the two samples (24% Sb and 4% As at Sb(1) for H3, *vs.* 22% Sb and 6% As at Sb(1) for H4, and 28% Sb and 1% As at Sb(2) for H3, and 20% Sb and 8% As at Sb(2) for H4).

Overall, it is remarkable how little the bond lengths and angles of the AlO_6 octahedral framework change in response to major substitutions, including vacancies, at the Al(1), Si, and Sb positions.

The FTIR spectra of samples A, S, and H4 in the 4000–450 cm^{-1} region are shown in Fig. 3*a*; a list of absorbance bands is given on the left side of Table 5. The spectra are similar to previously reported IR spectra of holtite and dumortierite (Voloshin *et al.*, 1977, 1987; Voloshin and Pakhomovskiy, 1988; Werding and Schreyer, 1990; Fuchs *et al.*, 2005). The right side of Table 5 lists absorbance peaks in holtite I, holtite II, and dumortierite from Voloshin *et al.* (1987) for comparison with the current spectra.

The spectra of samples A, S and H4 each show a series of peaks corresponding to OH stretching in the 4000–3000 cm^{-1} region (shown in Fig. 3*b*), confirming the presence of hydrogen in the holtite structure (see below). The spectrum of H4 also shows a small peak at 1648 cm^{-1} due to bending of non-structural H_2O (Voloshin *et al.*, 1987; Voloshin and Pakhomovskiy, 1988; Rossman, 1988).

Voloshin *et al.* (1987) and Voloshin and Pakhomovskiy (1988) compared several IR spectra of holtites with that of dumortierite, and identified certain peaks as characteristic of holtite I and holtite II, appearing in one variety but not the other. The spectra of A and S (holtite I) and H4 (holtite II) show both types of peaks. For example, Voloshin *et al.* (1987) and Voloshin and Pakhomovskiy (1988) identified peaks at 750 and 545 cm^{-1} as characteristic of holtite I, and peaks at 940–950 cm^{-1} and 825 cm^{-1} as characteristic of holtite II; however, all of these peaks appear to some degree in each of our three samples. Similarly, a side-peak at 1315 cm^{-1} on the main antisymmetric BO_3 stretching peak at 1360 cm^{-1}

is identified by Voloshin *et al.* (1987) and Voloshin and Pakhomovskiy (1988) as characteristic of holtite I, but only one (sample A) of our two holtite I samples show this feature (Fig. 3*c*). This suggests that holtite I and holtite II do not have distinct FTIR signatures.

The spectra of A, S and H4 each show a group of three small peaks around 2900 cm^{-1} which do not correspond to any peaks in the Voloshin *et al.* (1987) and Voloshin and Pakhomovskiy (1988) spectra. These may be due to C−O stretching in residue left behind after the samples were rinsed with ethanol and dried during preparation.

Water in holtite

Pryce (1971) measured 0.38 wt.% H_2O^+ and 0.08 wt.% H_2O^- in the type specimen, a holtite II, but the question whether H_2O is an essential constituent of holtite has remained unresolved. In dumortierite, OH is thought to occur primarily at the O(2) and O(7) positions (Moore and Araki, 1979; Alexander *et al.*, 1986; Werding and Schreyer, 1990; Ferraris *et al.*, 1995; Cempírek and Novák, 2005; Fuchs *et al.*, 2005). However, Hoskins *et al.* (1989) wrote that "...the (occupancy) factors obtained for O2 and O7...are in good agreement with the overall metal occupancy in Al1... For this reason there is not the need in holtite (as there is in dumortierite) for OH^- replacement of O^{2-} to provide a reduction in local charge to compensate for...a vacancy in Al1...". Nonetheless, there have been several reports of H_2O by infrared spectroscopy or single-crystal refinement. Voloshin *et al.* (1977) reported traces and 1.13 wt.% H_2O^+ in their 'anhydrous' and 'hydrated' varieties of holtite I from Voron'i Tundry, a distinction confirmed by IR evidence for OH in the latter, whereas Voloshin *et al.* (1987) reported IR evidence for H_2O (most likely as OH) in both holtite I and holtite II. Finding O(10) undersaturated in their refinement of holtite I from Voron'i Tundry, Kazantsev *et al.* (2005) concluded it was occupied by both O and OH. Kazantsev *et al.* (2006) calculated the occupancy to be 0.52 OH in a revision of the refinement.

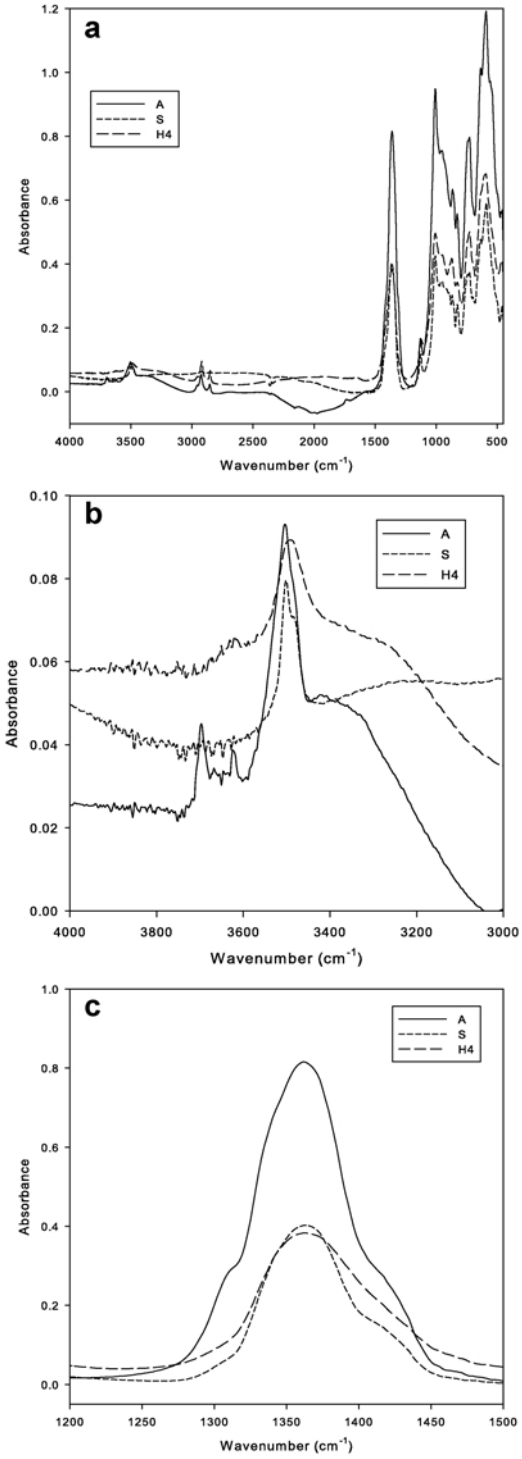

FIG. 3. FTIR spectra of samples A and S (both from Greenbushes, Western Australia) and H4 (from Szklary, Lower Silesia, Poland): (*a*) Full spectra; (*b*) 4000 cm^{-1} to 3000 cm^{-1} region showing OH stretching bands; (*c*) 1200 cm^{-1} to 1500 cm^{-1} region showing antisymmetric BO_3 stretching bands.

TABLE 5. Infrared absorption bands of holtite between 4000–450 cm^{-1}.

A (Australia) Holtite I	S (Australia) Holtite I	H4 (Poland) Holtite II	—— From Voloshin *et al*. (1987) —— Holtite I	Holtite II	Dumortierite
3697					3690
3625		3623*			3615
3504	3501	3490	3500–3510	3495–3500	3500
			3480		
		3400–3420		3400	
			3340		
2957	2957*	2954			
2925	2925	2919			
2854	2854	2850			
1727					
	1648	1630–1640	1650	1650	
1415	1415	1415	1415	1415–1420	1415
1362	1363	1363	1370	1360–1370	1375
1312			1315		
		1170	1165–1175	1170	
1128	1126	1121		1120–1125	
		1090–1095	1090–1095	1090	
				1045	
1007	1006	1006	1030–1020	1015	1015
952	952	950		940–950	
920†	920†			920–925	
893†	892	890†			
866	868	872	860–870	865–870	860
829	827	827		825	
		797–800		795	
		770–775	760–762	777	
742	743	744†	750		762
728	728	727	725	720–725	725
699†	698	698	695–700		700
636	636	635	635–640	650–652	640
			605–610		
591	589	592	590–600	585–590	590
558	561†	560†			
544†	538†	538†	545		535
497†	497†		520	500	
471	471†	472	465–470	460–462	470
459	459	458			

Peak positions are reported in cm^{-1}. Blank lines indicate a peak is absent in the corresponding spectrum.
* – very small peak, not visible in full spectrum shown in Fig. 3.
† – shoulder

Although charge-balance calculations based on our single-crystal structure refinements (see below) suggest that essentially no water is present, the FTIR results confirm that some OH is present in the samples measured. The peaks in the OH stretching region (Fig. 3*b*) closely resemble those reported for dumortierite (Fuchs *et al*., 2005; Werding and Schreyer, 1990). As noted by Rossman (1988) and Povarennykh (1978), the positions and integrated area of individual peaks in an IR spectrum depend on coordination and the local charge environment. Assuming OH is located at the O(2) and O(7) positions (each coordinated by one tetrahedral and two octahedral cations), Fuchs *et al.* (2005) identified the main dumortierite peak at 3495 cm^{-1} with a nine-charge coordination environment for OH, such as (Si^{4+}, Al^{3+}, $^{[6]}M^{2+}$)

or ($^{[4]}T^{3+}$, Al^{3+}, Al^{3+}). This is the largest OH peak in the holtite spectra, and it is located at 3501 cm^{-1} and 3504 cm^{-1} in the two Greenbushes samples A and S respectively, and at 3490 cm^{-1} in H4. If this peak is due to OH at O(2) and/or O(7), another nine-charge environment that must be considered is (Si^{4+}, $^{[6]}\square$, Ta^{5+}). Higher cation valences tend to shift absorbance peaks to higher wavenumbers, so the prevalence of this latter environment may be responsible for the shift to values above 3500 cm^{-1} in the Greenbushes samples. Other peaks identified in the IR spectrum of dumortierite by Fuchs *et al.* (2005) are the eight-charge environment such as (Si^{4+}, $^{[6]}M^{2+}$, $^{[6]}M^{2+}$) or (Si^{4+}, Ti^{4+}, $^{[6]}\square$) around 3620 cm^{-1}, the seven-charge environment (Si^{4+}, Al^{3+}, $^{[6]}\square$) at 3675 cm^{-1}, and the six-charge environment (Si^{4+}, $^{[6]}M^{2+}$, $^{[6]}\square$) at 3696 cm^{-1}. Spectra for samples A and H4 show small peaks near 3625 cm^{-1} which may correspond to the eight-charge environment, and sample A shows a peak at 3697 cm^{-1} which may correspond to the six-charge environment. The seven-charge environment peak is absent from all three spectra.

Chemical substitution and ordering in the holtite structure

Precession photographs synthesized from the X-ray data show diffuse layers mentioned by Pryce (1971) and Hoskins *et al.* (1989) normal to *a* at spacings of 2*a* and 3*a*. As mentioned previously, Hoskins *et al.* (1989) suggested that the diffuse layers indicate that although there is an ordering effect in any one individual tunnel, it is not strongly correlated with that of adjacent tunnels. What form might this ordering take?

In end-member anhydrous dumortierite, formula $Al_7BSi_3O_{18}$, all of the Al(1) sites are occupied by Al^{3+}. In holtite (and some dumortierite samples) at least some of the Al positions are occupied by pentavalent cations, mainly Ta^{5+} but sometimes Nb^{5+} as well. The substitution of pentavalent cations for Al^{3+} requires vacancies ($\square$) at some Al positions to maintain charge balance:

$$5Al^{3+} \rightarrow 3Ta^{5+} + 2\square \qquad (1)$$

The number of vacancies introduced at the Al sites by this substitution equals 2/3 the number of pentavalent cations at Al(1).

Independent of (Ta, Nb) content, when an Sb site is occupied, the nearby O(2) or O(7) site must be vacant. As substitution of an Sb^{3+} (or As^{3+}) ion at one Sb site obviates the octahedral coordination of oxygen atoms around the two adjacent Al(1) positions, it is likely that a complete replacement of SiO_4 rings by SbO_3 rings takes place, as is suggested by Hoskins *et al.* (1989). The structural channel in end-member dumortierite can be represented as a chain of Al^{3+} cations alternating with rings of three SiO^{2+} groups:

$$...(3SiO^{2+})(Al^{3+})(3SiO^{2+})(Al^{3+})(3SiO^{2+})...$$

A single SiO^{2+} ring in the channel is replaced by an Sb^{3+} ring as follows:

$$(3SiO^{2+})(Al^{3+})(3SiO^{2+})(Al^{3+})(3SiO^{2+}) \rightarrow (3SiO^{2+})(\square)(3Sb^{3+})(\square)(3SiOH^{3+}) \qquad (2)$$

This results in loss of coodination to the two adjacent Al(1) sites, which must now remain vacant. Hydrogen ions are added to oxygen atoms at three of the six coordinating O(2) and O(7) sites in order to maintain charge balance. Substitution 2 represents the insertion of a short $\square-$Sb segment into the Al−SiO chain. The $\square-$Sb segment can be expanded to preserve octahedral coordination for Al^{3+} (or other cations) by the following additional substitution:

$$(\square)(3SiOH^{3+})(Al^{3+})(3SiO^{2+}) \rightarrow (\square)(3Sb^{3+})(\square)(3SiOH^{3+}) \qquad (3)$$

A combination of substitution 2 followed by many substitutions 3 can create an arbitrarily long $\square-$Sb segment while introducing just three OH^- groups:

$$nAl^{3+} + 3nSiO^{2+} \rightarrow n\square + 3(n-1)Sb^{3+} + 3SiOH^{3+} \qquad (4)$$

In any given channel the amount of OH introduced by Sb-Si substitution is proportional to the number of $\square-$Sb chains, to a maximum of one OH per Sb (where substitution 2 acts alone). For very long $\square-$Sb chains (i.e. as $n \rightarrow \infty$), the amount of OH^- introduced in this fashion is negligible, and the average Sb-Si substitution is

$$Al^{3+} + 3SiO^{2+} \rightarrow \square + 3Sb^{3+} \qquad (5)$$

In total a number of vacancies equal to 1/3 of (Sb + As) are introduced at the Al(1) site. Note that these vacancies must necessarily be at Al(1) for coordination reasons.

Summing expression 4 over all $\square-$Sb chains in the structure results in the equation

$$nAl^{3+} + 3nSiO^{2+} \rightarrow n\square + 3(n-m)Sb^{3+} + 3mSiOH^{3+} \qquad (6)$$

where *n* is the total number of vacancies created and *m* is the total number of $\square-$Sb chains, with

TABLE 6. Holtite site compositions from X-ray diffraction structure refinement and stoichiometric analysis.

		H1	H2	H3	H4
Al(1) site	Al	0.55	0.56	0.46	0.62
		7.15	*7.28*	*5.98*	*8.06*
	Ta	0.32	0.32	0.26	0.11
		23.36	*23.36*	*18.98*	*8.03*
	□	0.13	0.12	0.28	0.28
Al(2) site	Al	1.97	1.99	1.99	2.00
		25.61	*25.74*	*25.87*	*26.00*
	□	0.03	0.01	0.02	0.00
Al(3) site	Al	1.97	1.98	1.99	2.00
		25.61	*25.74*	*25.87*	*26.00*
	□	0.03	0.02	0.01	0.00
Al(4) site	Al	1.83	1.86	1.94	1.93
		23.79	*24.18*	*25.22*	*25.09*
	□	0.17	0.14	0.06	0.07
Si, Sb sites	Si	2.61	2.64	2.15	2.18
		36.54	*36.96*	*30.10*	*30.52*
	Sb + As	0.39	0.35	0.84	0.82
		17.19	*15.33*	*41.94*	*38.22*
	O	17.61	17.64	17.15	17.18
		140.88	*141.12*	*137.20*	*137.44*
Total	Al	6.33	6.39	6.37	6.55
	□	0.36	0.29	0.37	0.35
	□ excl. Al1	0.23	0.17	0.09	0.07
Calculated*	Total Al	6.34	6.35	6.29	6.55
	Total □	0.34	0.33	0.45	0.34
	□ from Ta	0.21	0.22	0.17	0.07
	□ from Sb	0.13	0.12	0.28	0.27
	O	17.61	17.65	17.16	17.18

Site populations are given in a.p.f.u. and e.p.f.u. (in italics).
* Calculated based on refined Ta and Sb+As and the formula $Al_{7-5/3x-1/3y}Ta_x\square_{2/3x+1/3y}BSi_{3-y}(Sb,As)_yO_{18-y}$.

$m \leqslant n$. The OH groups are located at O(2) or O(7). Substitution 6 implies that anhydrous holtite has only a small number of very long □−Sb chains, so that $m << n$ and the equation reduces to substitution 5.

Given the above the formula of (Ta- and Nb-free) end-member holtite would be $Al_6B(Sb,As)_3O_{15}$. The channels would be completely empty (vacancies at all Al(1), Si(1), Si(2), O(2) and O(7) sites) which suggests that end-member holtite might be a useful molecular sieve.

If we assume that the above Ta-Al and Sb-Si substitutions are the only substitutions involved in transforming end-member dumortierite to holtite then we have a general holtite stoichiometry of

$$Al_{7-[5x+y+z]/3}(Ta,Nb)_x\square_{[2x+y+z]/3}BSi_{3-y}(Sb,As)_yO_{18-y-z}(OH)_z \quad (7)$$

where x is the total number of pentavalent cations, y is the total amount of Sb + As, and z is the total amount of OH, with $z \leqslant y$ ($z = y$ when all Sb rings are preceded and followed by Si rings). We ignore any di- and tetravalent cations substituting at the Al sites, tetrahedral substitutions at the Si or Sb sites, or additional anion substitutions. In particular, we neglect the Al(1) vacancy substitution mechanism $Al^{3+} + 3SiO^{2+} \rightarrow \square + 3SiOH^{3+}$

proposed by Moore and Araki (1978) for dumortierite, which corresponds to $z \geqslant 0$, $y = 0$ in formula 7. In addition, we have not considered the possibility of tetrahedral Al, which is reported in natural dumortierite, although rarely in excess of 0.15 Al per formula unit (Grew, 1996). Calculating holtite formulae assuming Si+Sb+As+P = 3 using the results of the microprobe analyses yields $z < 0$ for H4, and $z \sim y$ for H1, H2, H3, i.e. reasonable H_2O contents for the latter three holtite samples, but a negative H_2O content for H4. Assuming 0.122 Al in tetrahedral coordination gives $z = y = 0.919$ for H4, which corresponds to 1.28 wt.% H_2O. Thus, the presence of tetrahedral Al is plausible in H4, but not in holtite from Greenbushes or Voron'i Tundry.

Formula 7 with $z = 0$ (i.e. the anhydrous/long-chain case) agrees well with the site populations determined in the structure refinement, implying only small amounts of OH are present at the O(2) and O(7) sites. Table 6 summarizes the octahedral, total Si and Sb+As, and anion site populations determined from structural refinement and calculated from equation 6 using the refined Ta+Nb and Sb+As populations. Total Al and vacancy populations agree with calculated totals within ±0.08 a.p.f.u, with the largest discrepancy for sample H3. The calculation confirms that in all four samples the number of vacancies at Al(1) is equal to the number of vacancies due to Sb-Si substitution (equation 5). The number of vacancies created by Al-Ta substitution at Al(1) (equation 1), however, are distributed among the Al(2), Al(3) and Al(4) sites, with the greatest number at Al(4).

In the absence of Sb-Si substitution, the Al(1)−Al(1) distance is too short to allow pentavalent cations at adjacent Al(1) positions, so Al(1) positions containing Ta^{5+} or Nb^{5+} must be preceded and followed by vacant Al(1) sites. This is likely to be the situation in pentavalent-rich (or Ti^{4+}-rich) dumortierite. However, in holtite the vacancies due to Sb-Si substitution may provide enough separation between pentavalent cations to stabilize the channel without introducing additional vacancies.

The $Al(4)O_6$ octahedron is both edge- and face-sharing in its double chain. The cross-face Al(4)−Al(4) distance is 2.58−2.61 Å in the four samples, larger than the Al(1)−Al(1) distance but still smaller than cross-edge Al−Al distances. This makes Al(4) the most favourable site for octahedral vacancies aside outside of the Al(1) site.

The formula of holtite

Formula 7 with approximate values for x and y taken from the electron microprobe compositions and maximum z (= y) results in the following general formula for holtite I:

$$Al_{5.83}(Ta,Nb)_{0.50}\square_{0.67}BSi_{2.50}(Sb,As)_{0.50}O_{17.00}(OH)_{0.50}$$

and the following general formula for holtite II:

$$Al_{5.92}(Ta,Nb)_{0.25}\square_{0.83}BSi_{2.00}(Sb,As)_{1.00}O_{16.00}(OH)_{1.00}$$

Dumortierite, holtite I and holtite II: distinct species?

Our analyses of holtite I and holtite II confirm the distinct clustering of compositions in terms of the Si/(Sb+As) ratio reported by Voloshin *et al.* (1987) and Voloshin and Pakhomovskiy (1988), although the extremely limited number of localities for holtite (which effectively equates to a sampling limitation) may play a major role in the apparent clustering. That holtite I and holtite II occur together at both the type locality and at Voron'i Tundry, with no obvious intermediate compositions, could be interpreted to mean that these are two different minerals separated by a miscibility gap. Alternatively, the clustering of compositions could be due to genetic rather than crystallographic factors. In the Voron'i Tundry pegmatite, holtite I is a early phase forming prisms 0.3−5 cm long, whereas holtite II is typically finely fibrous (<1 mm) and later in the paragenetic sequence, replacing holtite I, stibiotantalite and microlite (Voloshin *et al.*, 1977, 1987; Voloshin and Pakhomovskiy, 1988). Differences in composition could have resulted from the different chemical environments in which crystals of the two holtite varieties formed. Further calling into question the presence of immiscibility is the smaller compositional gap between the two varieties in 390 analyses of holtite II from Szklary, which give a much greater range in the Si/(Sb+As) ratio (Pieczka, unpublished data). The crystal-structure refinements do not indicate a fundamental difference in cation ordering that might serve as a criterion for recognizing holtite I and holtite II as distinct species, and they would not qualify as distinct species using either the standard criterion that at least one site must be occupied by a different cation or anion or the new criterion of the dominant-valency rule (Hatert and Burke, 2008).

As noted above, dumortierite may contain significant Nb, Ta, As, Sb and Bi (Groat *et al.*, 2001; Cempírek and Novák, 2004; Borghi *et al.*, 2004; Vaggelli *et al.*, 2004**).** Are dumortierite and holtite separate species, or is holtite simply a Ta- and Sb-rich variety of dumortierite? Our results provide no evidence for a fundamental difference in formula, as Al is dominant at the Al(1) site and Si is dominant at the Si(1) and Si(2) positions in both minerals. Moreover, available analyses suggest the possibility of a continuum in the Si/(Sb + As) ratio between holtite I and dumortierite.

In conclusion, we recommend that use of the terms holtite I and holtite II be discontinued. A more precise definition of holtite and its distinction from dumortierite awaits detailed study of both minerals, including experiments to determine the maximum amount of As and Sb that can be accommodated in the dumortierite-holtite structure. Such a definition will have to address, or at least consider, differences in diffraction behaviour (i.e. presence or absence of superstructure maxima), not just changes in bulk chemistry.

Acknowledgements

The authors thank R. Pogson of the Australian Museum and P.W. Powhat from the National Museum of Natural History (Smithsonian Institution) for samples from the type locality, N. Yonson for help with data collection at UBC, G. Poirier for help with data collection at the Canadian Museum of Nature, R. Herbst-Irmer for help with twinning and E. Moffat for collecting the infrared spectra. The manuscript was improved by comments from an anonymous reviewer, Associate Editor E. Sokolova, and Editor M.D. Welch. Financial support was provided by the Natural Sciences and Engineering Research Council of Canada in the form of a Discovery Grant to LAG. The equipment in C-HORSE was purchased with the help of a grant from the Canadian Foundation for Innovation.

References

Alexander, V.D., Griffen, D.T. and Martin, T.J. (1986) Crystal chemistry of some Fe- and Ti-poor dumortierites. *American Mineralogist*, **71**, 786–794.

Armstrong, J.T. (1995) CITZAF: A package of correction programs for the quantitative electron microbeam X-ray analysis of thick polished materials, thin films, and particles**.** *Microbeam Analysis*, **4**, 177–200.

Borghi, A., Cossio, R., Fiora, L., Olmi, F. and Vaggelli, G. (2004) Chemical determination of coloured zoned minerals in 'natural stones' by EDS/WDS electron microprobe: an example from dumortierite quartzites. *X-ray Spectrometry*, **33**, 21–27.

Cempírek, J. and Novák, M. (2005) A green dumortierite from Kutná Hora, Moldanubicum, Czech Republic: spectroscopic and structural study. Pp. 4–5 in: *International Meeting Crystallization Processes in Granitic Pegmatites* (F. Pezzotta, editor). Elba, Italy, 2005, Book of Abstracts.

Creagh, D.C. and Hubbell, J.H. (1992) *International Tables for Crystallography, Vol C.* Kluwer Academic Publishers, Boston, USA, 200–206.

Creagh, D.C. and McAuley, W.J. (1992) *International Tables for Crystallography, Vol C.* Kluwer Academic Publishers, Boston, USA, 219–222.

Cromer, D.T. and Waber, J.T. (1974) *International Tables for X-ray Crystallography, Vol. IV.* The Kynoch Press, Birmingham, UK.

Ferraris, G., Ivaldi, G. and Chopin, C. (1995) Magnesiodumortierite, a new mineral from very-high-pressure rocks (Western Alps). Part I: Crystal structure. *European Journal of Mineralogy*, **7**, 167–174.

Fuchs, Y., Ertl, A., Hughes, J.M., Prowatke, S., Brandstätter, F. and Schuster, R. (2005) Dumortierite from the Gföhl unit: Lower Austria; chemistry, structure, and infra-red spectroscopy. *European Journal of Mineralogy*, **17**, 173–183.

Golovastikov, N.I. (1965) The crystal structure of dumortierite. *Soviet Physics Doklady*, **10**, 493–495.

Grew, E.S. (1996) Borosilicates (exclusive of tourmaline) and boron in rock-forming minerals in metamorphic environments. Pp. 387–502. in: *Boron: Mineralogy, Petrology, and Geochemistry.* (E.S. Grew and L.M. Anovitz, editors). Reviews in Mineralogy, **33**, Mineralogical Society of America, Chantilly, Virginia, USA.

Grew, E.S., Graetsch, H., Pöter, B., Yates, M.G., Buick, I., Bernhardt, H.-J., Schreyer, W, Werding, G, Carson, C.J. and Clarke, G.L. (2008) Boralsilite, $Al_{16}B_6Si_2O_{37}$, and 'boron-mullite': compositional variations and associated phases in experiment and nature. *American Mineralogist*, **93**, 283–299.

Groat, L.A., Grew, E.S., Ercit, T.S. and Piezcka, A. (2001) The crystal chemistry of dumortierite and holtite, aluminoborosilicates with heavy elements. *Geological Society of America Abstracts with Programs*, **33**, Abstract 383.

Groat, L.A., Grew, E.S., Ercit, T.S. and Pieczka, A. (2002) The crystal chemistry of holtite. *Abstracts of the 18th General Meeting of the International*

Mineralogical Association, p. 209.

Hatert, F. and Burke, E.A.J. (2008) The IMA–CNMNC dominant-constituent rule revisited and extended**.** *The Canadian Mineralogist*, **46**, 717–728.

Hoskins, B.F., Mumme, W.G. and Pryce, M.W. (1989) Holtite, $(Si_{2.25}Sb_{0.75})B[(Al_6(Al_{0.43}Ta_{0.27}\square_{0.30})O_{15}(O,OH)_{2.25}]$: crystal structure and crystal chemistry. *Mineralogical Magazine*, **53**, 457–463.

Ibers, J.A. and Hamilton, W.C. (1964) Dispersion corrections and crystal structure refinements. *Acta Crystallographica*, **17**, 781–782.

Kazantsev, S.S., Pushcharovsky, D.Yu., Pasero, M., Merlino, S., Zubkova, N.V., Kabalov, Yu.K. and Voloshin, A.V. (2005) Crystal structure of holtite I. *Crystallography Reports*, **50**, 42–47.

Kazantsev, S.S., Zubkova, N.V. and Voloshin, A.V. (2006) Refinement of composition and structure of holtite I. *Crystallography Reports*, **51**, 412–413.

Locock, A.J., Piilonen, P.C., Ercit, T.S. and Rowe, R. (2006) New mineral names. *American Mineralogist*, **91**, 216–224.

Moore, P.B. and Araki, T. (1978) Dumortierite, $Si_3B[Al_{6.750.25}O_{17.25}(OH)_{0.75}]$: a detailed structure analysis. *Neues Jahrbuch für Mineralogie Abhandlungen*, **132**, 231–241.

Pekov, I.V. (1998) Minerals first discovered on the territory of the former Soviet Union. Ocean Pictures, Moscow.

Pieczka, A. and Marszałek, M. (1996) Holtite – the first occurrence in Poland. *Mineralogia Polonica*, **27**, 3–8.

Platonov, A.N., Langer, K., Chopin, C., Andrut, M. and Taran, M.N. (2000) Fe^{2+}-Ti^{4+} charge-transfer in dumortierite. *European Journal of Mineralogy*, **12**, 521–528.

Pouchou, J.L. and Pichoir, F. (1985) "PAP" $\phi(\rho Z)$ procedure for improved quantitative microanalysis. *Microbeam Analysis*, 104–106.

Povarennykh, A.S. (1978) The use of infrared spectra for the determination of minerals. *American Mineralogist*, **63**, 956–959.

Pryce, M.W. (1971) Holtite: a new mineral allied to dumortierite. *Mineralogical Magazine*, **38**, 21–25.

Pryce, M.W. and Chester, J. (1978) Minerals of the Greenbushes Tinfield. *Mineralogical Record*, **9**, 81–84.

Rossman, G.R. (1988) Vibrational spectroscopy of hydrous components. Pp. 193–206. in: *Spectroscopic Methods in Mineralogy and Geology.* (F.C. Hawthorne, editor). Reviews in Mineralogy, **18**, Mineralogical Society of America, Chantilly, Virginia, USA.

Vaggelli, G., Olmi, F., Massi, M., Giuntini, L., Fedi, M., Fiora, L., Cossio, R. and Borghi, A. (2004) Chemical investigation of coloured minerals in natural stones of commercial interest. *Microchimica Acta*, **145**, 249–254.

Voloshin, A.V. and Pakhomovskiy, Ya.A. (1988) *Mineralogy of Tantalum and Niobium in Rare-Metal Pegmatites*. Nauka, Leningrad (in Russian).

Voloshin, A.V., Gordienko, V.V., Gel'man, Ye.M., Zorina, M.L., Yelina, N.A., Kul'chitskaya, Ya.A., Men'shikov, Yu.P., Polezhayeva, L.I., Ryzhova, R.I., Sokolov, P.B. and Utochkina, G.I. (1977) Holtite (first find in the USSR) and its relationship with other tantalum minerals in rare-metal pegmatites. *Novyye Mineraly i Pervyye Nakhodki v SSSR*, **106**(3), 337–347 (in Russian).

Voloshin, A.V., Pakhomovskiy, Ya.A. and Zalkind, O.A. (1987) An investigation of the chemical composition and IR-spectroscopy of holtite. in: *Mineral'nyye Assotsiatsii i Mineraly Magmaticheskikh Kompleksov Kol'skogo Polyostrova, Apatity, Kol'skiy Filial AN SSSR*, 14–34 (in Russian).

Werding, G. and Schreyer, W. (1990) Synthetic dumortierite: its PTX-dependent compositional variations in the system Al_2O_3-B_2O_3-SiO_2-H_2O. *Contributions to Mineralogy and Petrology*, **105**, 11–24.

Zubkova, N.V., Pushcharovskii, D.Yu., Kabalov, Yu.K., Kazantsev, S.S. and Voloshin, A.V. (2006) Crystal structure of holtite II. *Crystallography Reports*, **51**, 16–22.